Mass and Heat Transfer Evolutions of Ethanol Pool Fires under External Heat Flux

Yue H., Lizhong Y.*, Xiaodong Z., Yang P.

State Key Laboratory of Fire Science / University of Science and Technology of China, Hefei, Anhui, China

**Corresponding author's email: yanglz@ustc.edu.cn*

ABSTRACT

This paper focuses on quantifying experimentally the evolution of conduction, convection and radiation heat feedback mechanisms and corresponding mass burning rates of ethanol pool fires (8, 10, 12, and 15 cm diameter) under external heat fluxes ranging from 0 to 4.0 kW/m^2. The results show that the conduction heat feedback fraction is nearly independent of external heat flux, but decreases with pool diameter. Meanwhile, the contribution fractions of convection and radiation heat feedback mechanisms display a competitive relationship where the radiation heat feedback fraction increases with external heat flux while the convection heat feedback fraction changes in the opposite direction. The transitional external heat fluxes of the control regime are 3.3, 3.3, 2.8, and 1.3 kW/m^2 for 8, 10, 12, and 15 cm pool fires, respectively. The increment of the corresponding mass burning rate gradually declines in the convection-controlled regime, while is nearly constant in the radiation-controlled regime. The flame heat transfer blockage fraction β is introduced to express the variation of mass burning rate in the radiation-controlled regime based on a simple linear correlation. The heat blockage effect appears to be more significant for larger pool diameters given that the values of β are 0.008, 0.021, 0.056, and 0.128 for incremental pool diameters. Calculated mass burning rates based on the stagnant layer theory are in good agreement with the measured ones.

KEYWORDS: Heat feedback, burning rate, ethanol, pool fire, heat flux.

NOMENCLATURE

c_p	constant pressure specific heat (J/(kg·K))
y	vertical distance from bottom of pan (mm)
R	thermal resistance ((m^2·K)/W)
h	fuel thickness (m)
q''	heat flux (kW/m^2)
k	thermal conductivity (W/(m·K))
Δx	horizontal distance from inwall surface (m)
T	temperature (K)
A	area (m^2)
ΔH_v	heat of evaporation (kJ/g)
$\dot{m}''$	mass burning rate (kg/m^2·s)
X_r	flame radiation fraction
D	pan diameter (m)
γ	oxygen–fuel mass stoichiometric ratio (-)
φ	blocking factor (-)
χ	heat transfer fraction (-)
α	absorption coefficient (-)

Subscripts

cond	conduction
conv	convection
rad	radiation
ext	external
w	pan wall
l	liquid fuel
v	evaporation
r	pool radius

Proceedings of the Ninth International Seminar on Fire and Explosion Hazards (ISFEH9), pp. 704-715
Edited by Snegirev A., Liu N.A., Tamanini F., Bradley D., Molkov V., and Chaumeix N.
Published by St. Petersburg Polytechnic University Press
ISBN: 978-5-7422-6496-5 DOI: 10.18720/spbpu/2/k19-55

L effective heat of gasification (kJ/g)
h_c heat transfer coefficient (W/(m^2·K))

Greek

β flame heat transfer blockage fraction (-)

b boiling
0 initial values
g gas phase
es residual

INTRODUCTION

The total energy required to evaporate the liquid fuel before burning derives from either the internal heat energy of the liquid fuel or from the external heat energy transferred to the liquid. For a steady burning pool fire, this evaporation energy results from three heat feedback mechanisms, namely conduction (through the pan wall), convection and radiation of the flame [1, 2]. The three flame heat feedback mechanisms essentially control the mass burning rate of a pool fire [1-5]. The evolution of the heat feedback mechanisms depends on numerous factors, such as pool diameter [3], pool bottom temperature [4], wind conditions [5] and so on. As for environmental conditions that affect the material combustion, external heat flux, imposed by hot walls, smoke and gases or adjacent burning objects, appears to be of significant importance in the situation of compartment and enclosure fires [6]. This addition of external heat flux is the key to disastrous fire growth [7] since heat feedback can promote fire growth in special configurations.

The presence of external heat fluxes enhances the radiative heat feedback to the fuel. In this process, the soot and gas mixture existing between the flame sheet and the fuel surface emit and absorb the radiative heat flux [8], meanwhile the convection heat feedback is inhibited due to the "blowing" effect [5] of evaporated fuel just above the fuel surface. However, to our knowledge, there are limited studies on pool fire behaviour under external heat flux [6, 9-11], where the prominent one has been contributed by Zhang [9, 10]. It concluded that the increase rate of burning rapidly decreased as the flame volume and radiation blockage effect increased, but the evolution of the interactive relationship of mass burning rate and heat feedback of pool fires are still not clear with external heat fluxes addition. J. Quintiere [11] presented theoretical formulations of steady burning rate with external radiant heating based on an idealized liquid model. A critical heat flux (CHF) for burning was determined by the intercept of a linear equation (according to heat transfer analysis) and the abscissa, but this theory was only applicable when the external heat flux was much larger than the critical heat flux for burning. A wide range of external heat fluxes was lacking and still needed further investigation.

This paper aims to quantify experimentally the evolutions of three heat feedback mechanisms with circular pool diameters of 8, 10, 12, and 15 cm. The external heat fluxes range from 0 to 4.0 kW/m^2. The corresponding mass burning rates are discussed with respect to the change of the dominant heat feedback mechanisms accordingly and formalized in simple correlations in the radiation-controlled regime. Furthermore, calculated mass burning rates based on heat transfer analysis by a stagnant layer theory solution are compared to the experimental data.

EXPERIMENTAL DESIGN

Experimental facility

Figure 1 shows the experimental setup constructed for this study. The radiant heater consists of eleven silicon carbide rods, insulated by mullite at the top and on both sides. These heating elements, with near-grey-body radiation characteristics, have a stable high emissivity (0.8-0.9) in the wavelength range of 2-15 μm [12], which includes the absorption spectrum of ethanol pool fire flame [13]. The surface size of the radiation heating source is 530 mm×530 mm. The top of the

radiant heater has three rows of smoke ventilation circular holes which let the gas and smoke vent through by natural convection without accumulation. The external radiant fluxes received by the fuel surface were obtained by varying the electric power supplied to the radiant panels. Radiation calibration tests were performed before the pool fire tests, and the result shows that the difference in radiant flux between the center and the edge of the 15 cm pool diameter was within $\pm 2\%$, which verifies the uniformity of the radiation. The variation in the external heat flux ranges from 0 to 4.0 kW/m^2.

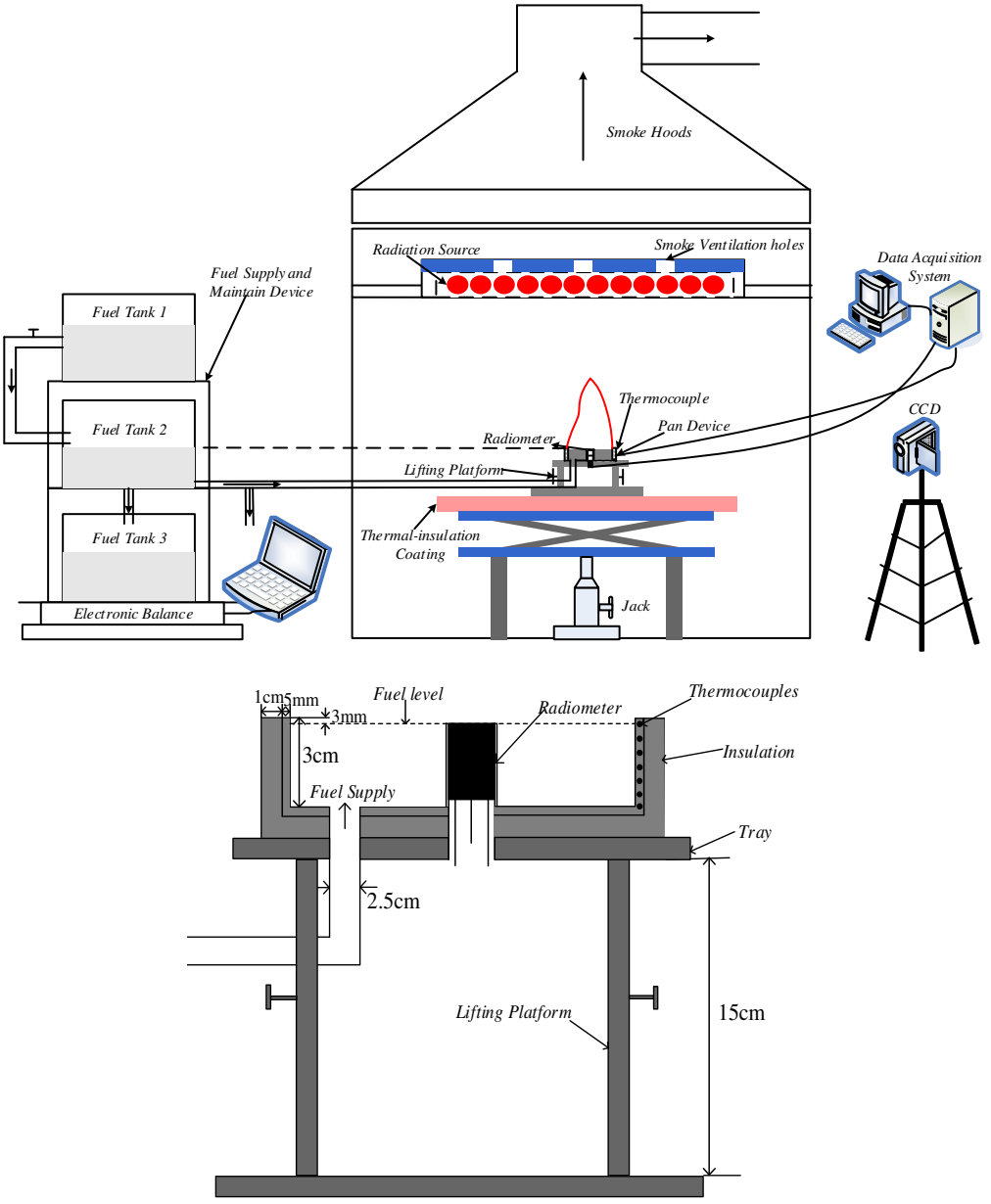

Fig. 1. Schematic diagram of experimental facility.

Experiments were performed with laboratory-scale ethanol pool fires. The circular pans were made of steel with diameters of 8, 10, 12, and 15 cm in order to investigate scale effects. The wall height and thickness of the pan were 3 cm and 5 mm with a lip height of 3 mm maintained by a fuel leveling device [14] during the experiment. The pans were placed horizontally on the adjustable lifting platform right below the radiation source. The side and bottom walls were wrapped in a double-layer fiberglass fabric (1 cm thick) and aluminum foil to reduce the heat loss and avoid the influence of lateral and bottom heating especially under external heat flux. The distance between the radiation source and the sample was set at 50 cm to leave enough space for the whole flame. The fuel mass loss was measured once a second by an electronic balance (Sartorius Co. Ltd) with accuracy of 0.1 g. The experiments were repeated three times to ensure good repeatability and the measurement time was extended to at least 10 minutes to guarantee experimental stability.

Measurement of conduction feedback

The quantification of conduction feedback was based on temperature measurements at the wall and the adjacent fuel. With a view to the symmetrical characteristics of circular pans, seven pairs of thermocouples with tilting arrangement were sheathed into holes (1 mm diameter) drilled along the vertical wall. The thermocouples for wall temperature were embedded into blind holes with a horizontal distance of 1 mm away from the inner wall surface, while those for the adjacent fuel temperature were embedded into penetrable holes, which were 5 mm horizontally away from the inner wall surface, as shown in Fig. 2. The temperature data were recorded when steady state was achieved, at which point the maximum standard deviation was within 2□. The local heat conduction flux can be estimated from the method introduced in Ref. [4, 15] considering both conduction within the wall and heat transfer to the fuel, as portrayed in Eq. (1).

$$\dot{q}''_{cond}(y) = \frac{T_w(y) - T_l(y)}{R_w + R_l}, \tag{1}$$

where $\dot{q}''_{cond}(y)$ is wall heat flux along the vertical wall (kW/m^2). $R_w = \Delta x_1 / k_w$ ((m^2·K)/W) and $R_l = \Delta x_2 / k_l$ ((m^2·K)/W) are wall and fuel thermal resistances, respectively, and $\Delta x_1 = 1$ mm and $\Delta x_2 = 5$ mm. k_w and k_l are the thermal conductivities of the wall and the fuel, which are set as 16.8 and 18 W/(m·K), respectively.

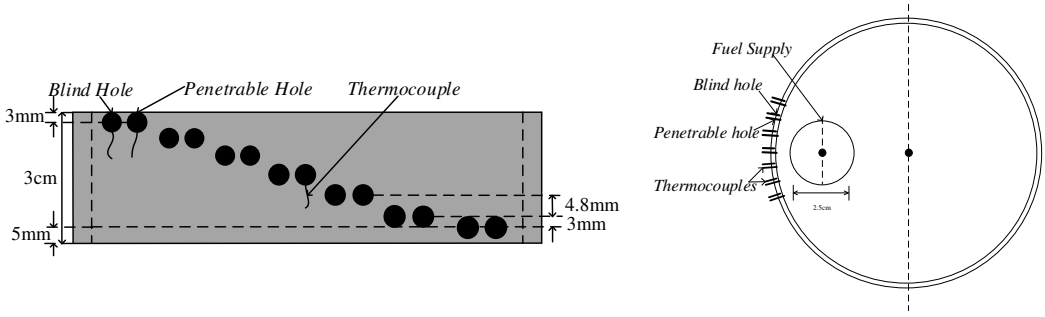

Fig. 2. Thermocouple setup for temperature measurement of wall and adjacent fuel (a) side view (b) top view.

The conduction feedback can then be estimated from the integration of the wall heat flux through the pool area in symmetrical configuration:

$$\dot{q}''_{cond} = \left(A_w / A_p\right) \int_0^h (1/h)\, \dot{q}''_{cond}(y)\, dy, \tag{2}$$

where $A_w = \pi DL$ and $A_p = \pi D^2/4$, h refers to the constant fuel thickness (27 mm), D is the pool diameter (m). The wall conduction feedback fraction can then be expressed as:

$$\chi_{cond} = \dot{q}''_{cond} / \dot{m}'' L , \tag{3}$$

where $L = c_{p,l}(T_b - T_0) + \Delta H_v$ is effective heat of gasification (kJ/g), $\dot{m}''$ is mass burning rate (kg/(m^2·s)), $c_{p,l}$ is the specific heat capacity (2.4 kJ/(kg·K)) [16], ΔH_v is heat of evaporation (kJ/g), set as 0.837 kJ/g [17]. T_b and T_0 are boiling temperature (351.6 K) [18] and initial fuel temperature (298.2 K), respectively.

Measurement of radiation feedback

The radiation heat feedback received by the liquid surface exhibits a certain distribution in the radial direction [1, 19]. Thus, circular pans were divided into multiple independent annular regions for radiation measurement, as shown in Fig. 3. A series of experiments was carried out by means of three identically water-cooled Schmidt-Boelter radiometers (SGB, view angle: 150°, measurement range: 0-20 kW/m^2, diameter: 18 mm, wavelength range: 0.3-50 μm, uncertainty: 3%), located at different radii along the radial direction. In addition, quartz plates (diameter: 2.2 cm, thickness: 0.2 cm) were used to cover the surface of the radiometer in order to eliminate the effect of condensation of combustible vapors. The transmissivity calibration coefficient of the quartz plates is 0.452 according to the measurement of the ratio of incident radiation heat flux to the sensor with and without the plate.

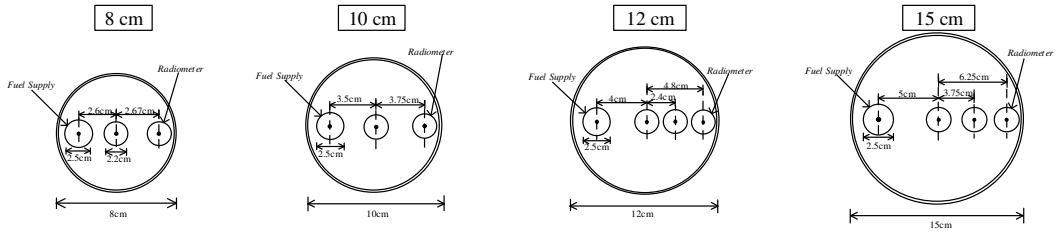

Fig. 3. Schematic diagram of radiation measurement along the pan radius.

The mean radiation heat feedback received by the combustible fuel surface is subsequently integrated to obtain the radiant heat flux to the entire surface.

$$\dot{q}''_{rad} = \frac{8}{D^2}\int_0^{D/2} \dot{q}''_r(r) r dr , \tag{4}$$

where $\dot{q}''_r(r)$ is the radiant heat flux measured along the radius (kW/m^2). The radiation feedback fraction similarly is calculated as:

$$\chi_{rad} = \dot{q}''_{rad} / \dot{m}'' L . \tag{5}$$

Calculation of convection feedback

The convection feedback fraction can be expressed as:

$$\chi_{conv} = 1 - (\chi_{cond} + \chi_{rad}) . \tag{6}$$

RESULTS AND DISCUSSION

Conduction heat feedback of side wall to fuel

The time-averaged evolution of side wall and adjacent fuel temperatures of a representative 12 cm ethanol pool fire is exemplified in Fig. 4. It should be noted that the bottom surface of the wall is located at $y = 0$ mm and the top is at $y = 27$ mm, flush with the fuel level. It is apparent that distinct thermal structures along the vertical wall and the adjacent fuel show a synchronous variation trend, in which both temperatures have an almost exponential increase from bottom to top because the top of the wall is close to the flame and the bottom is subjected to the supplying cooling fuel. However, the profiles of thermal gradients become more uniform under increasing external heat fluxes due to the intense heating effect of both external heat flux and flame. Subsequently, it is obvious that these vertical temperature distributions are attributed to the coupling interactions between conduction inside the steel wall and heat transfer to the fuel. The temperature variation data agree well with those of Ref. [4].

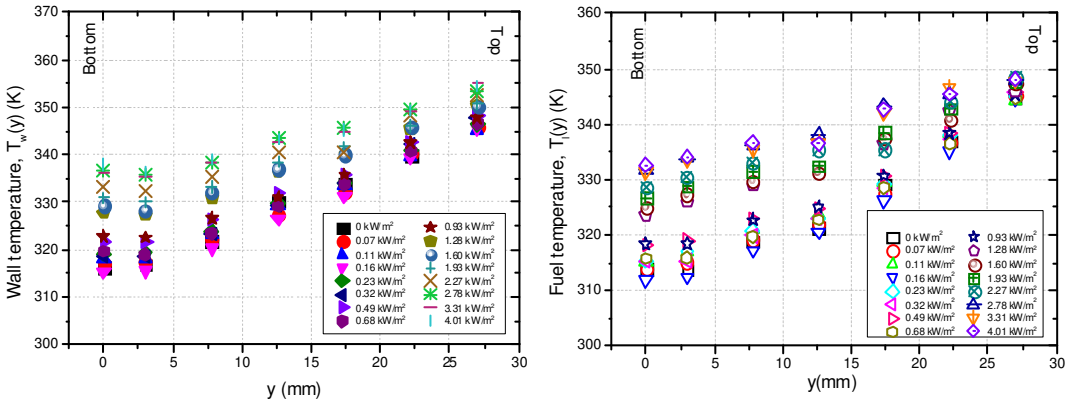

(a) (b)

Fig. 4. Temperature distributions along the longitudinal wall direction of 12 cm pool fires. (a) wall temperature; (b) adjacent fuel temperatures.

Based on Eq. (1) and Eq. (2), the overall conduction heat feedback can be calculated from the integrated wall heat flux scaled to the area of the pan, as presented in Fig. 5 for all experimental conditions. The conduction heat feedback has an increasing trend with the external heat flux owing to increasing radiative heat to the wall rim, while it decreases with pool diameter.

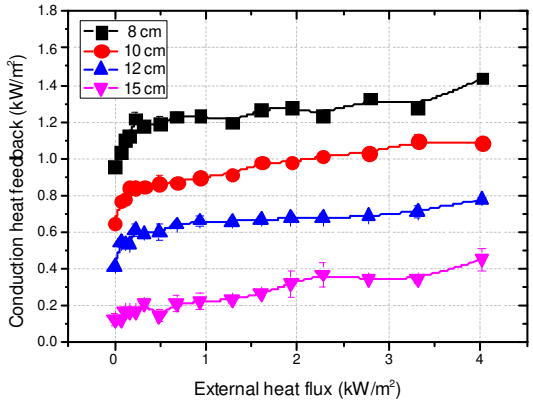

Fig. 5. Evolution of conduction heat feedback of side wall.

RADIATION HEAT FEEDBACK FROM FLAME TO FUEL SURFACE

By measuring the incident radiation heat flux along the radial direction, the experiments of 12 cm pool fires are used as examples to show the evolution. As shown in Fig. 6, the incident radiation heat flux $\dot{q}_r''(r)$ decreases as the position changes from the center to the edge within the experimental uncertainty, consistent with the variation trends reported in the literature [1, 19]. By extrapolating the incident radiant heat flux over the whole pool surface, the resulting mean radiation heat feedback can be estimated according to Eq. (4), as demonstrated in Fig. 7. The mean radiation heat feedback increases notably with external heat flux. These increments, however, are narrowed for higher external heat flux. The declining increase amplitude of radiation feedback results from the complicated changes of flame volume and soot fraction, which cause a considerable radiation blockage effect, and this effect is more conspicuous for larger pool fires.

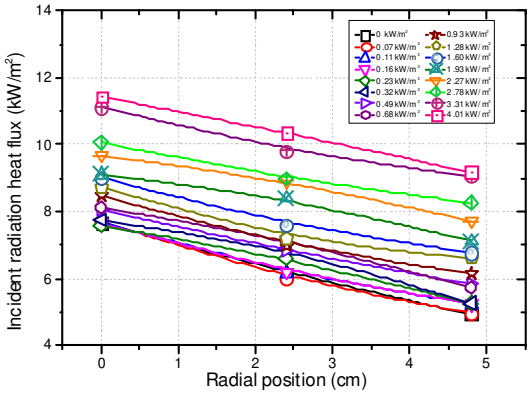

Fig. 6. Evolution of radiation heat flux along radial direction of 12cm pool fires.

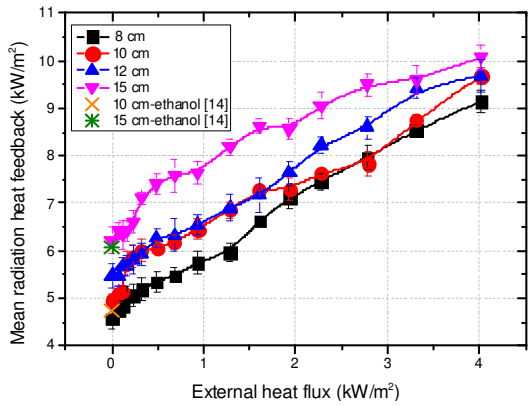

Fig. 7. Evolution of mean radiation heat feedback.

Evolution of heat feedback and corresponding mass burning rate

The mass burning rates of pool fires depend on total evaporation energy $\dot{m}''L$, which is supplied by heat feedback by conduction $\dot{q}''_{cond}$, convection $\dot{q}''_{conv}$ and radiation $\dot{q}''_{rad}$. It should be noted that reflection and reradiation from the fuel surface have been neglected for simplicity as these terms are small in comparison to the received flame heat feedback. The coupled contributions of these three heat feedbacks basically result in the non-monotonous change of $\dot{m}''$ and the dominant feedback mechanisms are connected to the flame scale and external heat flux, as illustrated in Fig. 8, where the left Y-axis is the measured mass burning rate under experimental conditions, while the right Y-axis denotes the heat transfer fraction (conduction, convection and radiation) based on Eqs. (3), (5) and (6). The following observations can be made:

(1) The conduction heat fraction appears to be nearly constant under different external heat fluxes with negligible contribution, while these values gradually decrease when the flame scale becomes larger. Basically, the variations of the conduction heat fraction reveal that the contribution of fuel vaporization is nearly unaffected by conduction, while convective and radiative heat feedback to the fuel surface become more dominant for relatively larger pool diameters.

(2) Under no external heat flux, convection heat feedback is dominant for all pool diameters. Convection and radiation heat feedback exist in a competitive relationship; however, the external heat flux represent an increasing contribution to total radiation heat feedback as it gradually

becomes more intense, while the contribution of convection heat feedback becomes less and less important. Physically, the attenuation of convection heat feedback is a consequence of expansion of fuel-rich volume and Stefan flow [20] immediately above the fuel surface due to increasing mass burning rates. Transition external heat fluxes, referring to the shift of convective to radiative mechanisms, are 3.3, 3.3, 2.8, and 1.3 kW/m^2 respectively, for 8, 10, 12, and 15 cm pool fires, meaning that the influence of external heat flux is more perceptible for larger pool fires.

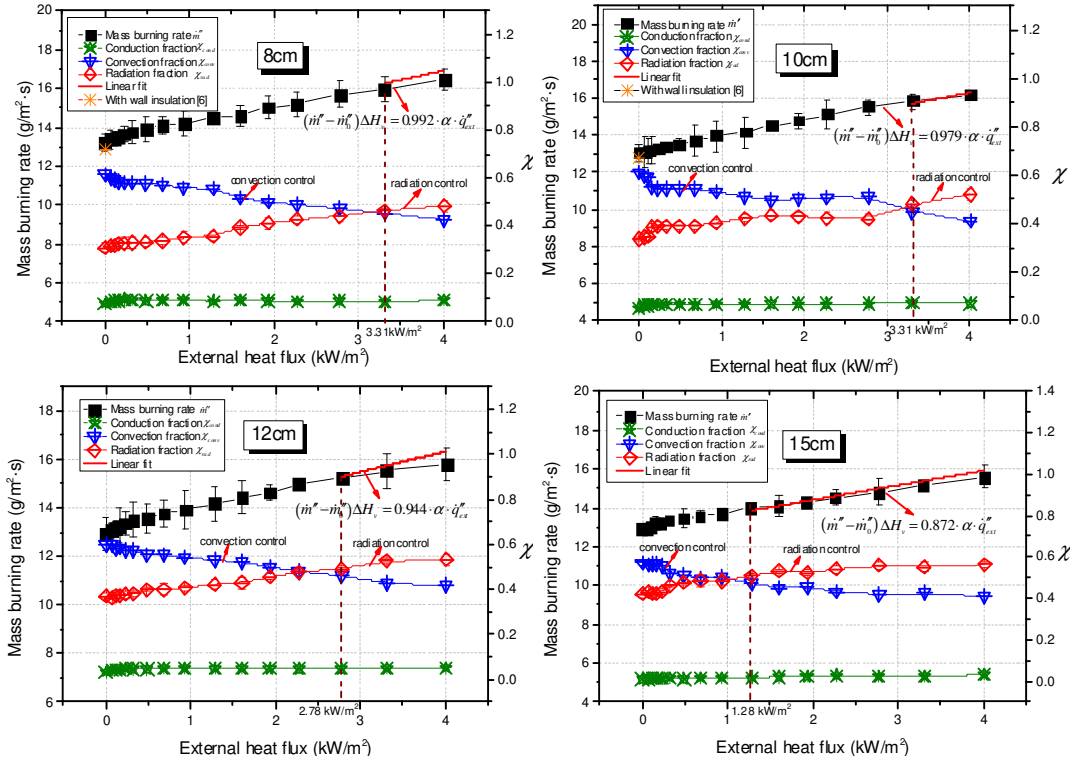

Fig. 8. Dependent relationships of mass burning rate with external heat flux and flame scale.

(3) With regard to the variations of heat transfer mechanisms, the mass burning rate $\dot{m}''$ initially experiences an exponential growth in the convection-controlled regime. Beyond the transition external heat fluxes, radiation heat feedback clearly becomes dominant. A linear variation can be seen in Fig. 8. Considering a part of the radiation energy is emitted by the gas and soot through the flame, and the radiation energy is transmitted to the fuel and helps the fuel evaporation. The deviation of the evaporation energy under or no external heat flux is ascribed to the external heat flux being absorbed by the fuel. Consequently, by introducing a constant flame heat transfer blockage fraction β, which denotes the total energy loss under external heat fluxes, the linear equation can be expressed as Eq. (7) according to the formulation in PMMA fires [21]:

$$\beta = 1-\left(\dot{m}''-\dot{m}_0''\right)L/\left(\alpha\dot{q}_{ext}''\right), \tag{7}$$

where $\dot{m}_0''$ is mass burning rate under no external heat flux (g/(m^2·s)), $\dot{q}_{ext}''$ is external heat flux (kW/m^2), ΔH_v is heat of evaporation (kJ/g), α is the energy absorption coefficient, which is set as 0.84 [22]. The slope of the linear equation is $(1-\beta)\alpha/L$ and the intercept yields $\dot{m}_0''$. The values of β for 8, 10, 12, and 15 cm pool fires are 0.008, 0.021, 0.056 and 0.128, respectively, which reveals

that the heat transfer blockage effect is more significant for larger pool diameters. For pool diameters of 8 cm, the evaporation energy roughly equals to the combination of the flame heat feedback and external heat flux in the radiation-controlled region.

Finally, for purely convection-dominated pool fires, the mass burning flux (burning rate per unit surface area) can be correlated by the stagnant layer theory [23]:

$$\dot{m}'' = \left(k_g / c_{p,g}\delta\right)\ln\left(1+B\right), \tag{8}$$

where k_g and $c_{p,g}$ are gas-phase thermal conductivity (W/(m·K)) and specific heat capacity (J/(kg·K)), which are thermophysical properties of the fuel vapor at the film temperature $\left(T_f + T_b\right)/2$. T_f is the experimentally measured flame temperature, almost independent of pan diameters and external heat fluxes, which equals 1326 K with radiation error calibration. δ is thickness length scale of the convection boundary layer. B is the dimensionless mass transfer number:

$$B = \left[Y_{O_{2,\infty}}\left(\Delta H_c/\gamma\right) - c_{p,g}\left(T_b - T_\infty\right)\right]\Big/ L, \tag{9}$$

where $Y_{O_{2,\infty}}$ is the mass fraction of oxygen in the ambient, ΔH_c is heat of combustion, γ is the oxygen–fuel mass stoichiometric ratio, T_∞ denotes the ambient temperature. For a convective boundary layer, the heat transfer coefficient, h_c, is approximately equal to k_g/δ [7], thus Eq. (8) can be transformed to:

$$\dot{m}'' = \left(h_c / c_{p,g}\right)\ln\left(1+B\right). \tag{10}$$

With consideration of the heat transfer balance, the steady mass burning rate can be correlated by Eq. (9) and Eq. (10), combined with inclusion of radiative and conductive transfer effects:

$$\dot{m}''L = \left(h_c/c_{p,g}\right)\left[\varphi\Big/\left(e^{\varphi}-1\right)\right]\cdot\left[Y_{O_{2,\infty}}\Delta H_c/\gamma\left(1-X_r\right) - c_{p,g}\left(T_b - T_\infty\right)\right] + \alpha\left(\dot{q}''_{f,r} + \dot{q}''_{es}\right) + \dot{q}''_{cond}, \tag{11}$$

where $\varphi = c_{p,g}\dot{m}''/h_c$ refers to the blocking factor [7]. The flame radiant fraction, X_r, is accounted for by the representative value of 0.2 [24]. $\dot{q}''_{f,r}$ is the flame radiation to the fuel surface (kW/m^2), $\dot{q}''_{es}$ is the residual radiation heat flux after $\dot{q}''_{ext}$ passing through the flame, and measured $\dot{q}''_{rad}$ is the sum of $\dot{q}''_{f,r}$ and $\dot{q}''_{es}$. In Eq. (11), reflection and reradiation are also neglected for simplicity.

An empirical correlation is adopted to obtain approximate solutions for the convective heat transfer coefficient, h_c, based on a horizontal plate in natural convection configurations with two dimensionless numbers $Nu = h_c x/k_g$ and $Ra = \left(\nu_g/\alpha_g\right)\left(g\beta_g x^3\left(T_f - T_b\right)\right)\Big/\nu_g{}^2$ [25]:

$$h_c = k_g Nu/x = \left(k_g C/x\right)\left(g\beta_g \Delta T x^3/\left(\nu_g\alpha_g\right)\right)^n, \tag{12}$$

$$\begin{aligned} &C = 0.54, n = 1/4 \left(10^4 \le \mathrm{Ra} \le 10^7\right) \\ &C = 0.15, n = 1/3 \left(10^7 \le \mathrm{Ra} \le 10^{11}\right) \end{aligned}, \tag{13}$$

where x denotes the characteristic length, which is equal to the pan diameter for pool fires D. ΔT is the difference between the film and pool surface temperature. β_g and ν_g are the volume thermal expansion coefficient for an ideal gas and dynamic viscosity. α_g is thermal diffusivity, which can be obtained as $\alpha_g = k_g / \rho_g c_{p,g}$. ρ_g is gas-phase density, estimated as $\rho_g = PM/RT$, $(M \approx 29)$. It is worth noting that values of k_g, β_g and ν_g are dependent on film temperature, which can be estimated from Ref. [26].

By substituting measured $\dot{q}''_{rad}$ and $\dot{q}''_{cond}$ into Eq.(11), the theoretical $\dot{m}''$ can be calculated iteratively. Calculated $\dot{m}''$ are compared against the measured values for all experimental conditions conducted in this study as shown in Fig. 9. The dashed and dashed/dotted lines represent $\pm 10\%$ and $\pm 5\%$ deviation from the solid line, respectively. It can be seen that the majority of calculated $\dot{m}''$ is within the $\pm 5\%$ deviation from the measured values. The aforementioned energy balance analysis is validated against the measured values.

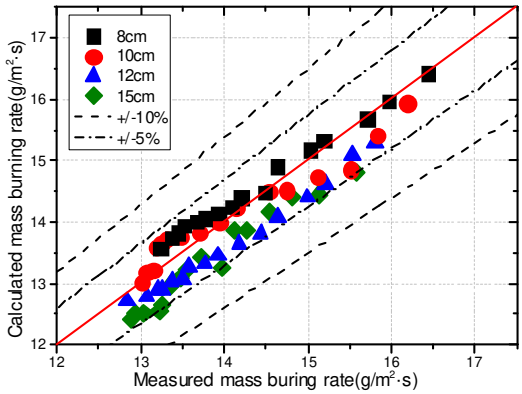

Fig. 9. Calculated mass burning rates in comparison with the measured values.

CONCLUSIONS

This paper presents the evolutions of heat feedback and corresponding mass burning rate of ethanol pool fires under external heat fluxes. Direct measurements of conduction and radiation heat feedback are experimentally realized. The corresponding mass burning rates are analysed based on the heat feedback estimates. The major findings are summarized as follows:

1) The contribution of conduction heat feedback is insignificant ($\chi_{cond} < 0.1$) in the current experimental conditions. The conduction feedback slightly increases with increasing external heat flux, but shows a decreasing trend for larger pool diameters.
2) Radiation heat feedback increases gradually with external heat flux, while this increase attenuates for larger scale pools and higher external heat fluxes.
3) Under no external heat flux, convection heat feedback is dominant for all experimental conditions. When exposed to external heat fluxes, radiation heat feedback fractions gradually increase while convection heat feedback fractions exhibit opposite variations. The transition external heat fluxes, marking the change of dominant regimes, are 3.3, 3.31, 2.8, and 1.3 kW/m^2, respectively for 8, 10, 12, and 15 cm pool fires in this experiment.
4) The mass burning rate experiences a decreasing trend to increase in the convection-controlled regime, then maintains a stable increment in the radiation-controlled regime.

The flame heat transfer blockage fractions β are 0.008, 0.021, 0.056 and 0.128 for 8, 10, 12, and 15 cm pool fires in the radiation-controlled regime, which is interpreted to mean that the flame blockage effect depends upon the flame scale and is more perceivable for larger pool diameters.

5) A stagnant layer theory based on heat transfer analysis is proposed to characterize the mass burning rate. Experimental data are well in accordance with calculated data.

ACKNOWLEDGMENTS

This work was supported by the National Science Foundation of China (No.51636008), Key Research Program of Frontier Sciences, CAS (No. QYZDB-SSW-JSC029), and the Fundamental Research Funds for the Central Universities (No. WK2320000035).

REFERENCES

[1] A. Hamins, S.J. Fischer, T. Kashiwagi, M.E. Klassen, J.P. Gore, Heat Feedback to the Fuel Surface in Pool Fires, Combust. Sci. Technol. 97 (1994) 37-62.

[2] A. Nakakuki, Heat transfer mechanisms in liquid pool fires, Fire Saf. J. 23 (1994) 339-363.

[3] V. Blinov, G. Khudiakov, US Army Translation NTIS No, AD296762, 1961.

[4] A. Vali, D.S. Nobes, L.W. Kostiuk, Quantifying the Conduction Pathways in a Laboratory-Scale Methanol Pool Fire, Combust. Sci. Technol. 187 (2015) 765-779.

[5] L. Hu, J. Hu, S. Liu, W. Tang, X. Zhang, Evolution of heat feedback in medium pool fires with cross air flow and scaling of mass burning flux by a stagnant layer theory solution, Proc. Combust. Inst. 35 (2015) 2511-2518.

[6] A. Nasr, S. Suard, H. El-Rabii, J.P. Garo, L. Gay, L. Rigollet, Heat feedback to the fuel surface of a pool fire in an enclosure, Fire Saf. J. 60 (2013) 56-63.

[7] J.G. Quintiere, Fundamentals of fire phenomena, John Wiley Chichester, 2006.

[8] L. Orloff, J. De Ris, M.A. Delichatsios, Radiation from Buoyant Turbulent Diffusion Flames, Combust. Sci. Technol. 84 (1992) 177-186.

[9] X. Zhang, J. Vantelon, P. Joulain, A. Fernandez-Pello, Influence of an external radiant flux on a 15-cm-diameter kerosene pool fire, Combust. Flame 86 (1991) 237-248.

[10] X. Zhang, P. Joulain, Thermal radiation from a small-scale pool fire: influence of externally applied radiation, Combust. Flame 92 (1993) 71-84.

[11] J. Quintiere, A theoretical basis for flammability properties, Fire Mater. 30 (2006) 175-214.

[12] Y. Zhou, L. Yang, J. Dai, Y. Wang, Z. Deng, Radiation attenuation characteristics of pyrolysis volatiles of solid fuels and their effect for radiant ignition model, Combust. Flame 157 (2010) 167-175.

[13] J.M. Suo-Anttila, T.K. Blanchat, A.J. Ricks, A.L. Brown, Characterization of thermal radiation spectra in 2m pool fires, Proc. Combust. Inst. 32 (2009) 2567-2574.

[14] L. Hu, S. Liu, L. Wu, Flame radiation feedback to fuel surface in medium ethanol and heptane pool fires with cross air flow, Combust. Flame 160 (2013) 295-306.

[15] L.M. Jiji, L.M. Jiji, Heat convection, Springer, 2006.

[16] P. Zhu, X. Wang, C. Tao, Experiment study on the burning rates of ethanol square pool fires affected by wall insulation and oblique airflow, Exp. Therm. Fluid Sci. 61 (2015) 259-268.

[17] A. Nakakuki, Heat transfer in pool fires at a certain small lip height, Combust. Flame 131 (2002) 259-272.

[18] D. Drysdale, An introduction to fire dynamics, John Wiley & Sons, 2011.

[19] A. Bouhafid, J. Vantelonf, Radiative heat flux and energy balance at the surface of a small-scale kerosene pool fire, Prog. Astron. Aeron. (1991) 297-313.

[20] A. Vali, Investigation of the transport phenomena within the liquid phase of a methanol pool fire, in, Ph. D. Thesis, University of Alberta, Canada, 2014.

[21] Z. Li, N. Liu, X. Xie, L. Zhang, X. Guo, R. Tu, Heat transfer blockage effect of small-scale PMMA flame under exterior heat radiation, Int. J. Therm. Sci. 122 (2017) 26-32.

[22] A. Luketa, Assessment of Simulation Predictions of Hydrocarbon Pool Fire Tests, Report SAND2010-2511, Sandia National Laboratories, Albuquerque, NM, (2010).

[23] D.B. Spalding, The combustion of liquid fuels, Proc. Combust. Inst. 4 (1953) 847-864.

[24] J. Gore, M. Klassen, A. Hamins, T. Kashiwagi, Fuel property effects on burning rate and radiative transfer from liquid pool flames, Fire Saf. Sci. 3 (1991) 395-404.

[25] T.L. Bergman, F.P. Incropera, D.P. DeWitt, A.S. Lavine, Fundamentals of heat and mass transfer, John Wiley & Sons, 2011.

[26] J. Gong, Y. Chen, J. Jiang, L. Yang, J. Li, A numerical study of thermal degradation of polymers: Surface and in-depth absorption, Appl. Therm. Eng. 106 (2016) 1366-1379.